Tip Steering for Fast Imaging in AFM

Submitted to the 2005 American Controls Conference

Sean B. Andersson
Division of Engineering and Applied Sciences
Harvard University
Cambridge, MA 02138
sanderss@deas.harvard.edu

Jiwoong Park
The Rowland Institute
Harvard University
Cambridge, MA 02138
park@rowland.harvard.edu

Abstract— **In atomic force microscopy a sharp tip, supported by a cantilevered beam and interacting locally with a sample, is raster-scanned over a surface to build a three-dimensional image. Typical scan times are on the order of minutes or longer, depending on the size, resolution, and image quality desired. For a variety of reasons it is of great interest to reduce the time to gather an image, with applications including the imaging in real time of dynamic phenomena such as the motion of single molecules in molecular biology. In many cases the sample to be imaged is string-like, such as nanowires, actin, and DNA strands. In this case most of the imaging time is wasted gathering data about the substrate rather than about the sample. In this work we propose a high-level control algorithm to steer the tip along the string, thereby imaging only the area directly around the sample. This approach focuses the resolution directly where desired and greatly reduces the time to gather an image by minimizing the area to be scanned. Depending on the sample, an order of magnitude or better reduction in the imaging time can be achieved. As the algorithm makes no demands on the low-level control of the tip it can be combined with approaches aimed at increasing the allowed scanning speed, resulting in even greater reductions in the imaging time. Furthermore, the chances of damaging the tip due to interaction with stray particles on the substrate is greatly reduced since the tip is kept near to the sample. We present a physical experiment in which a carbon nanotube is imaged using an atomic force microscope controlled by the tip-steering algorithm. To the authors knowledge this is the first reported instance of an image obtained by such high-level feedback control.**

I. Introduction

Scanning probe microscopy (SPM) is a class of atomic-scale imaging technologies in which a tip, interacting locally with a sample, is raster-scanned over the surface to build a three-dimensional image. A variety of different physical principles can be used for imaging with examples including scanning tunneling microscopy (STM) which measures the electron tunneling current between the tip and the sample [4], near-field scanning optical microscopy (NSOM) which provides resolution beyond the diffraction limit of the illuminating light [8], atomic force microscopy (AFM) which measures the surface repulsion forces [3], and magnetic resonance force microscopy (MRFM) which measures the forces due to the magnetic nuclei in the sample [21]. Work in this area is ongoing and new technologies are continuing to be developed.

Because the measurement is local, the tip must be scanned over the surface and an image built over time. With the raster-scan pattern, typical imaging times can be on the order of several minutes or longer, depending on the size, resolution, and quality of image desired. While this long time delay is merely an inconvenience when imaging static structures, it is a fundamental problem when using SPM to investigate dynamic phenomena. Due to the wide variety and importance of such phenomena, particularly in molecular biology, it is of great interest to reduce the time to capture an image.

In AFM, a sharp tip, supported by a cantilevered beam, is brought in close contact with the sample and the deflection of the beam is measured. The microscope can be operated in several modes including contact (constant-height) mode, constant-force mode, and tapping mode. AFM is particularly well-suited for the investigation of biological structures because it requires no special material properties of the sample, it operates in liquid, and it has high spatial resolution [17]. In this paper we focus on AFM as the target application. However the general algorithm developed is applicable to all SPM technologies.

A variety of methods have been proposed to reduce the imaging time in AFM. Most initial methods modified the design of the microscope such as using cantilevers with very high natural frequency [18] or controlling the quality factor of the probe [1], [13]. Most commercial machines control the lateral and vertical motion of the tip utilizing simple PI control loops and recent work has used advanced feedback control to speed up the scanning system [7] and modern model-based control methods to increase the bandwidth of the AFM in the vertical direction [14], [15].

A few researchers have developed innovative techniques for imaging dynamic phenomena in molecular biology using an atomic force microscope, such as the transcription of DNA by RNA polymerase [9], [11]. Sequential AFM images, separated by between 37 seconds to 2 minutes, were compared to determine the activity of RNA polymerase. However, RNA polymerase has been shown to translocate along natural double stranded DNA templates at a maximal speed of between 12 and 19 bases per second during transcription [12] and thus this approach is far from imaging

the transcription of a single base. In order to achieve this goal, new control techniques are needed.

Often the sample of interest has a structure which is string-like with examples including nanowires, DNA strands, actin strands, and microtubules. In this case, under the raster-scan approach much of the imaging time is wasted in gathering data about the substrate rather than about the sample. In this work we seek to minimize the imaging time by using a high-level control algorithm to steer the tip along the string. Modeling the sample as a planar curve, we seek to perform a "local" raster-scan by moving the tip along a line segment which is perpendicular to the curve as given by the local frame defining the curve. Using ideas from curvature-based control [10], [19], the next scan line is determined by estimating the next position of the frame from the current data.

This approach provides several benefits. The time to acquire an image is greatly reduced simply by reducing the total area that needs to be covered by the tip. Depending on the type of sample being imaged, an order of magnitude or better improvement in the scanning time can be expected. In addition, the approaches reduces the likelihood of damage to the tip due to stray particles on the surface. Moving the tip over these large structures can easily damage the tip; by keeping the tip local to the string it is less likely that these structures will be encountered. Furthermore, the approach developed is a high-level algorithm which makes no demands on the low-level control of the tip. It can therefore be combined with other techniques to achieve even greater reductions in imaging time.

II. Basics of AFM

We give here a very basic description of AFM. See, e.g. [2], for a more detailed introduction. The basic structure of an atomic force microscope is shown in Figure 1. The system is fully actuated in x, y, z with most machines utilizing a separate actuator for the z direction. In addition many modern microscopes have an independent actuator to drive the tip for tapping mode (described below). The x, y, and z positions may be directly measured and fed back to the controller or may be controlled in an open loop fashion. When the tip is brought in proximity to the sample surface, interaction forces cause the supporting beam to bend. This deflection is measured through the use of an optical lever in which a laser beam is reflected off the cantilever and onto a split photo-diode. The controller itself is connected to a host computer which typically displays the data and sends scan parameters such as the scan size and scan speed as well as high level commands such as start and stop. In most commercial devices the low level controller implements a high-speed PI controller, although as discussed in Section I researchers have developed more advanced control techniques.

Most images are acquired using one of three modes. In *contact* or *constant force* mode the tip is brought into stable contact with the sample. As the tip moves across

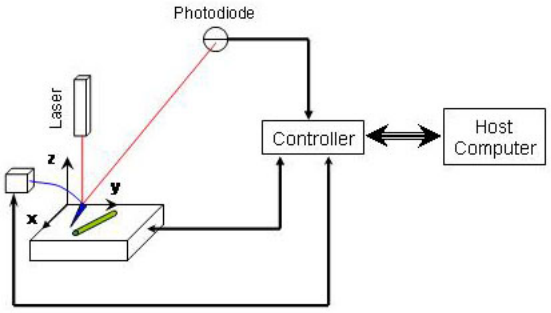

Fig. 1. Atomic force microscope schematic

the sample it is deflected up or down due to topographic variations in the sample. This deflection is directly measured by the microscope and the controller actuates the z-direction to maintain a constant deflection in the beam. Since the cantilever behaves as a linear spring, the interaction force can be determined from the deflection measurement. In *tapping* mode the tip is driven into near-resonance and then brought close enough to the sample so that it contacts the surface at the bottom oscillation cycle. Due to changes in the topography, the oscillation amplitude and phase is changed. The controller uses the output of the optical lever and actuates the $z-$ direction to maintain a constant oscillation amplitude. Because the tip is not in constant contact with the surface, lateral forces applied by the tip to the sample are minimized. This can be especially important when imaging soft biological samples both to prevent damage to the sample and to produce an accurate image. Finally, in *non-contact* mode the tip is once again driven into resonance. It is then brought close to, but not in actual contact with, the surface. The motion of the tip is influenced by the short range noncontact forces of the sample and topography is sensed by detecting changes in the tip motion. Because it requires a high resonance frequency, this imaging mode is used almost exclusively for imaging in air.

III. Local raster-scanning

A. The algorithm

We model the string-like sample as a planar curve whose spatial evolution is given by the dynamic equations for the Frenet-Serret frame. In the plane, this frame is defined by the tangent vector to the curve at a point and a choice of normal direction perpendicular to the tangent vector. Such a frame is shown in Figure 2 superimposed on an image of a DNA strand captured with an AFM operated in tapping mode.

Let s denote arclength along the curve. The equations of motion for the frame are given by

$$\begin{aligned} r'(s) &= q_1(s), \\ q_1'(s) &= \kappa(s) q_2(s), \\ q_2'(s) &= -\kappa(s) q_1(s), \end{aligned} \tag{1}$$

where $r(s)$ is the point in the plane on the curve at arclength s, $q_1(s)$ and $q_2(s)$ are the tangent and normal vectors at s,

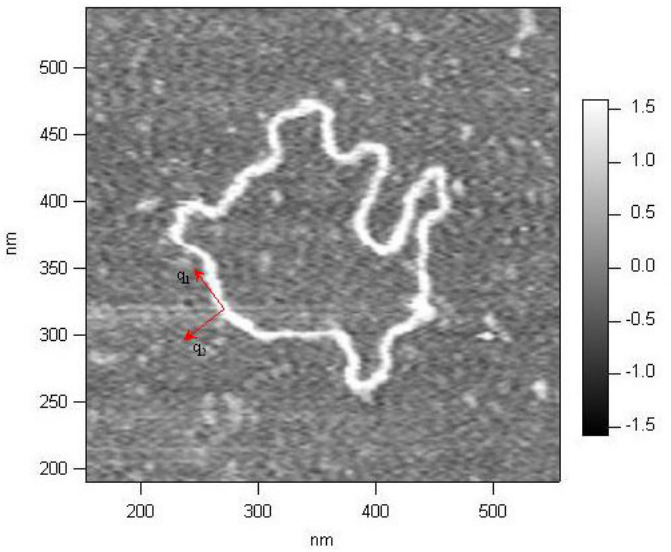

Fig. 2. Frenet-Serret frame superimposed on an AFM image of a DNA strand

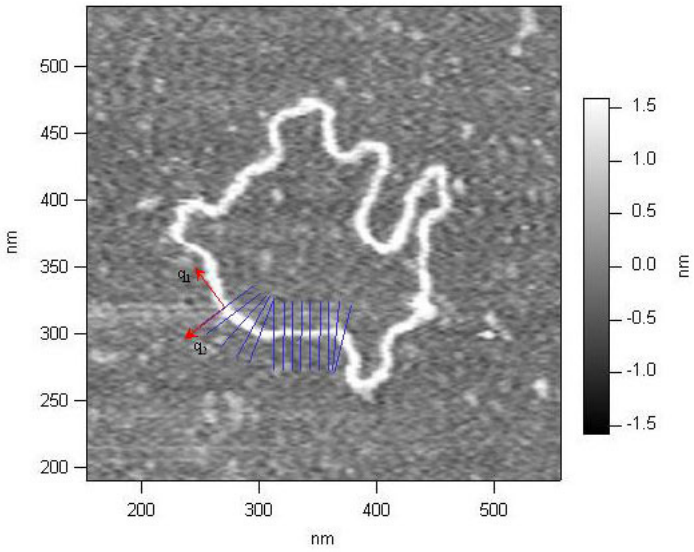

Fig. 3. Local raster-scanning.

$\kappa(s)$ is the curvature at s, and $'$ indicates derivative with respect to arclength. We assume that the initial conditions $r(0), q_1(0)$, and $q_2(0)$ are given.

To scan this sample we wish to imitate the raster scan motion but ensure that each scanline crosses the string perpendicular to the tangent vector q_1 and that the midpoints of each scanline lie on $r(s)$. Let v denote the desired scan speed and let a denote the desired width of the scan. If the underlying curve were known, then given a position $r(s)$ on the curve and the normal vector $q_2(s)$ at that point, the desired path of the tip is given by

$$\dot{x}(t) = \pm v q_2(s), \quad x(0) = r(s), \quad t \in \left[-\frac{a}{2v}, \frac{a}{2v}\right] \tag{2}$$

where the sign of the derivative indicates the direction of crossing. We can then step forward a desired length Δ along the curve and repeat the process. This approach is illustrated in Figure 3. Because the image produced depends not only on the geometry of the sample but also the geometry of the tip and the direction of the scan over the sample, in most cases it is best to always scan the tip across the sample in the same direction rather than alternating scan directions despite the additional time this introduces.

The path of the underlying curve is of course not known a priori. It can however be estimated local to a point $r(s)$ given the current Frenet-Serret frame and the curvature at s by appealing to the spatial evolution equations in (1). We assume that κ changes slowly with respect to the step size Δ. The position $r(s)$ can be detected from the output of the AFM using a variety of estimation methods, depending on the type of sample being imaged. For example, one could utilize an observer-based sample detection scheme developed by Sebastian, Sahoo, and Salapaka [16] to rapidly detect the edges of the sample and then take $r(s)$ as either edge or as the midpoint.

Given estimates for two adjacent points on the string, $\hat{r}(s-\Delta)$ and $\hat{r}(s)$, the tangent vector $q_1(s)$ can be estimated using a simple finite difference approximation, that is

$$\hat{q}_1(s) = \frac{\hat{r}(s) - \hat{r}(s - n\Delta)}{\|\hat{r}(s) - \hat{r}(s-\Delta)\|} \tag{3}$$

where $\|\cdot\|$ denotes the standard Euclidean metric. Here n is a fixed integer that can be chosen to offset difficulties arising from the small positional differences between points when the step size along the string is small. As the pair $q_1(s), q_2(s)$ are always orthogonal, $\hat{q}_2(s)$ is given by simply rotating $\hat{q}_1(s)$ by $\frac{\pi}{2}$ radians. Any noise in the measurement of $r(s)$ is of course amplified in this estimate of derivative.

To estimate the curvature we use a geometric approach based on Heron's formula (see [5] for a derivation and detailed description of the following). Let A, B, C be three successive and nearby points on a curve and denote the Euclidean distances between the points as a, b, c respectively, as in Figure 4. The radius of curvature of the circle is then

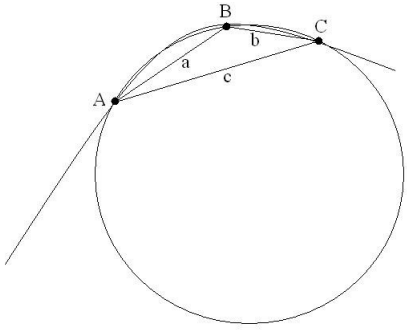

Fig. 4. Curvature approximation (from [5])

$$\kappa(A,B,C) = \pm 4\frac{\sqrt{l(l-a)(l-b)(l-c)}}{abc} \tag{4}$$

where $l = \frac{1}{2}(a+b+c)$ is the semi-perimeter of the triangle. The estimate of the curvature of the string at the point $r(s)$ is given by (4) where the points A, B, C correspond to $r(s-2n\Delta), r(s-n\Delta)$, and $r(s)$ respectively where again n is a fixed integer. (See [20] for more information on curvature estimation.) The sign is positive if the cosine of the angle between the vector connecting the points $r(k-n)$ and $r(k)$ and the normal vector is positive (so that the normal vector points "inside" the curve).

Given these estimates of the parameters for the Frenet-Serret frame at the arclength s the next position $r(s+\Delta)$ and tangent vector $q_1(s+\Delta)$ can be estimated by solving (1). Since the curvature is assumed to change slowly with respect to the step size along the string, we may approximate it as constant along the interval Δ. The solution to (1) for fixed κ and for step size Δ is given by a simple application of the variation of constants formula. The resulting update equations are

$$r(s+\Delta) = \begin{cases} \frac{A_1(\kappa(s)\Delta)}{\kappa(s)} \begin{bmatrix} q_1(s) \\ q_2(s) \end{bmatrix} + r(s), & \kappa \neq 0 \\ q_1(s)\Delta, & \kappa = 0 \end{cases} \tag{5}$$

$$\begin{bmatrix} q_1(s+\Delta) \\ q_2(s+\Delta) \end{bmatrix} = A_2(\kappa(s)\Delta) \begin{bmatrix} q_1(s) \\ q_2(s) \end{bmatrix} \tag{6}$$

where

$$A_1(\theta) = \begin{bmatrix} \sin(\theta) & 0 & 1-\cos(\theta) & 0 \\ 0 & \sin(\theta) & 0 & 1-\cos(\theta) \end{bmatrix} \tag{7}$$

and

$$A_2(\theta) = \begin{bmatrix} \cos(\theta) & 0 & \sin(\theta) & 0 \\ 0 & \cos(\theta) & 0 & \sin(\theta) \\ -\sin(\theta) & 0 & \cos(\theta) & 0 \\ 0 & -\sin(\theta) & 0 & \cos(\theta) \end{bmatrix} \tag{8}$$

The basic algorithm described above is summarized as follows.

Algorithm 3.1: Local raster-scanning:

0. Initialize $r(0), q_1(0), q_2(0), \kappa(0)$, and set $k = 0$, $m = 1$.
1. Set $s = k\Delta$.
2. For $t \in \left[-\frac{a}{2v}, \frac{a}{2v}\right]$ control x as in (2)
3. Measure $r(s)$ and estimate $q_1(s), q_2(s), \kappa(s)$
4. Estimate the next position of the curve using (6)
5. Set $k = k+1$ and go to 1.

B. Discussion

To consider the reduction in imaging time possible using this algorithm, consider the DNA image in Figure 2. The image is approximately 500 nm square and thus, to obtain a 2 nm lateral resolution, 250 scan lines are required using the traditional raster-scan pattern. If the tip moves at 1 $\frac{\mu m}{s}$ (2 lines per second) the image will require 125 seconds to obtain. The total length of the DNA strand in the image is roughly 1 μm. Moving in steps of 2 nm along the strand, 500 steps are required to image the entire DNA using the local raster-scan approach. DNA is only a few nanometers in diameter and to ensure each scan line fully crosses the strand, assume each scan line is 20 nm in length. If the tip is moved at the same speed as during the traditional raster-scan then each line will take 20 ms to complete and thus the entire DNA strand will be imaged in only 10 seconds.

The algorithm relies on two main assumptions. First, the change in the curvature of the sample between each scan line must be small since the algorithm assumes it is constant over the step size Δ. If this assumption does not hold then the next predicted scan line will not cross the sample and the algorithm will fail. An example of this behavior in simulation is shown in Figure 5. It is thus important that the step size remain small. However, a small step size is required to produce high resolution images and thus this assumption is not overly restrictive. In addition, one can increase the length of the scan line to ensure that the sample is crossed. However, as the length of the scan line increases it becomes more likely that other samples will be encountered and thus this approach must be handled with some care.

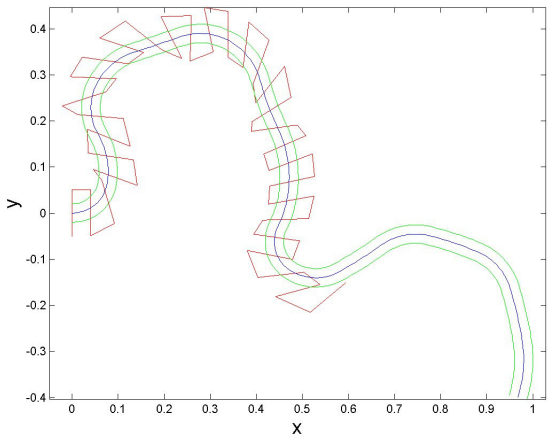

Fig. 5. Effect of step size

The second assumption is that the estimation of the center position of the sample is accurate. Any error in the measurement of $r(s)$ will be greatly amplified in the estimates of the tangent vector and curvature and the algorithm will not be able to track the sample. See [6] for additional comments along these lines. However, detection and estimation techniques can be used to improve the estimate and make the algorithm more robust to noise.

IV. Simulations and Experiments

A. Simulation

To initially verify the algorithm we performed a simulation experiment utilizing data of DNA acquired from an atomic force microscope using the traditional raster-scan

technique and shown in Figure 2. We note that a plane-fit was performed on the data to remove the offsets in the height measurement which vary across different scan lines. It was assumed that the measurement was corrupted with zero mean Gaussian noise. To estimate the edges of the DNA strand from the height data a maximum likelihood estimator was used to determine whether a measurement was on the string or off the string. Under the assumption that the string had a rectangular cross section, the estimator stated that a given measurement was on the string if the height exceeded half the maximum height in the scan (assumed to be the height of the string) and otherwise the measurement was assumed to be of the substrate. To prevent chattering due to the fact that the string was not rectangular, a majority rule was used over a small window of measurements around the sample point. Once the edges of the strand were detected, the center was found by taking the midpoint.

In Figure 6 we show the results of the tracking algorithm with the trajectory of the tip shown superimposed on the AFM image. In Figure 7 we show the (simulated) height data acquired by the algorithm. The algorithm tracks the DNA strand fairly well so long as the change in curvature from step to step remains relatively small. The performance of the algorithm in this example appears to be limited primarily by the granularity of the original sampling. Due to this granularity, the measurements of the center of the string and the estimates of the tangent and curvature are fairly rough. So long as the curvature remains fairly small the algorithm is still able to track quite well. However when the strand has a rapid turn, as on the upper left edge of the strand in Figure 6, the algorithm loses the string. While in practice a large magnitude curvature can be accommodated with smaller steps along the string, in this data set the sampling size is fixed and reducing the step size in the simulation beyond the sampling size does not produce finer measurements.

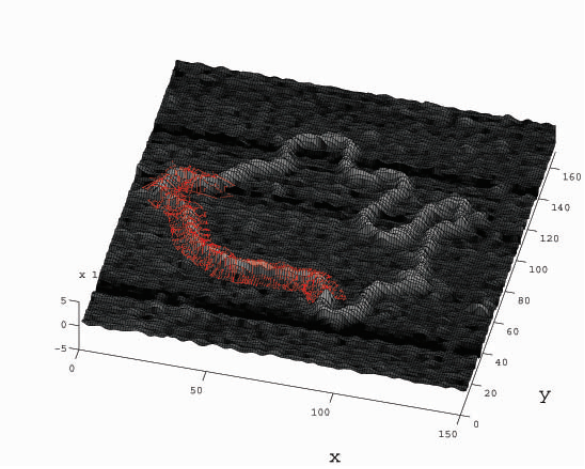

Fig. 6. AFM data and tracking trajectory

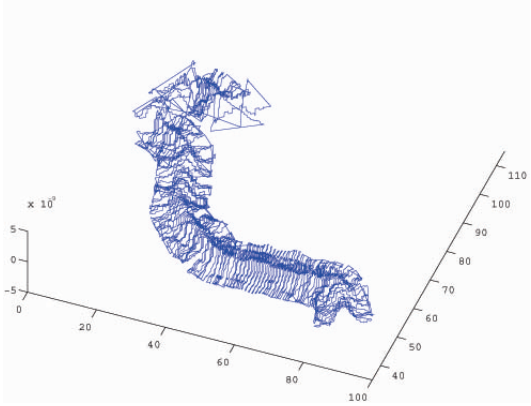

Fig. 7. Data from tracking algorithm alone

B. Experiments

Physical experiments were also performed using a MFP-3D AFM system from Asylum Research. The algorithm was implemented in WaveMetrics' Igor Pro environment and interfaced to the high-level control software of the microscope. While this allowed the algorithm to be implemented quickly, it introduced lengthy communication delays (on the order of 100-200 ms) between each line scan. As a result the experiments achieved only modest reductions in scan times. However they do serve to illustrate the effectiveness of the technique. The microscope was operated in tapping-mode in air in all experiments.

In Figure 8 we show an image of a carbon nanotube obtained using the traditional raster-scan pattern. The image is 826 nm square with 256 scan lines and 256 points along each line, yielding a lateral resolution of approximately 3.2 nm. The tip velocity was approximately 4 $\frac{\mu m}{s}$ and the image was gathered in approximately 50 s. Notice that two short sections along the nanotube are missing. Over most of its length the tube is 1-2 nm tall.

The local raster-scan algorithm was initialized with a frame near the lower end (in y) of the nanotube, immediately above the lower missing section. A scan width of 80 nm, a step size of 6 nm, and a scan speed of 5 $\frac{\mu m}{s}$ were specified. Care was taken to ensure that the initial scan line completely crossed the nanotube but the initial conditions were otherwise not precisely matched to the sample. As in the simulation, a maximum likelihood estimator was used to determine the edges of the nanotube from the height data. In Figure 9 a typical profile for a scan across the nanotube is shown. As an alternative to the height data one can use the amplitude of the oscillation. As the tip encounters a raised surface, the oscillation amplitude first decreases until the low-level controller has time to adjust the z-position. Similarly, as the tip moves off the raised surface, the oscillation amplitude will momentarily increase. The peaks in this pattern, shown in Figure 10, provide a direct measurement of the edges. This method works quite well for tall, rigid structures where the peaks are much larger than

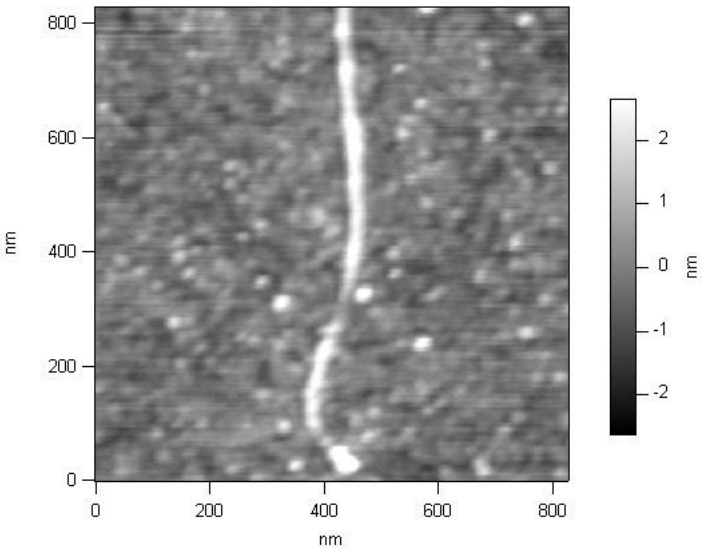

Fig. 8. Image of carbon nanotube using traditional raster-scan.

the measurement noise. For smaller samples, such as the missing sections along the nanotube, this method produced extremely poor measurements of the string edges. We note that a more robust method, such as in [16], should produce better results.

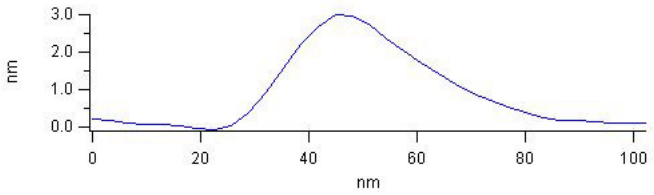

Fig. 9. Typical height profile of the nanotube.

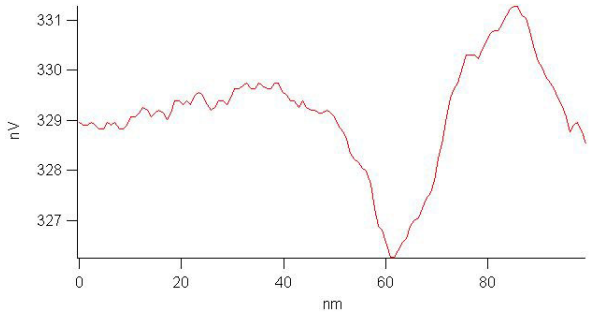

Fig. 10. Typical tip oscillation amplitude profile.

Along the missing sections of the nanotube the measurements produce random locations for the string. Thus, to help the algorithm move through these sections and to help smooth the overall path, both the heading direction as defined by the orientation of the tangent vector with respect to a fixed frame and the curvature were digitally filtered using a four-pole type I Chebyshev filter. In Figure 11 we show the path of the tip along each scan. Note that along the regions where the height of the nanotube is particularly low the spacing of the scan lines is not uniform and the heading angle varies greatly from scan to scan. However once the scan crosses the nanotube again the algorithm locks on. Notice also that there is one scan line which is greatly shifted with respect to the rest. This was due to a small particle very close to the nanotube which resulted in a shifted estimate of the center position of the tube. The algorithm recovered well soon after this anomaly. In Figure 12 we show both the raw curvature determined using Heron's formula and the filtered curvature.

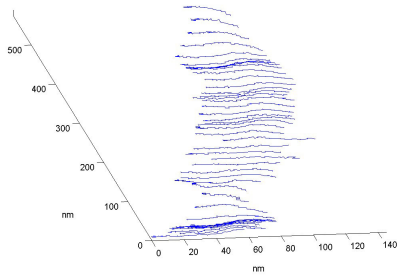

Fig. 11. Line scans along carbon nanotube.

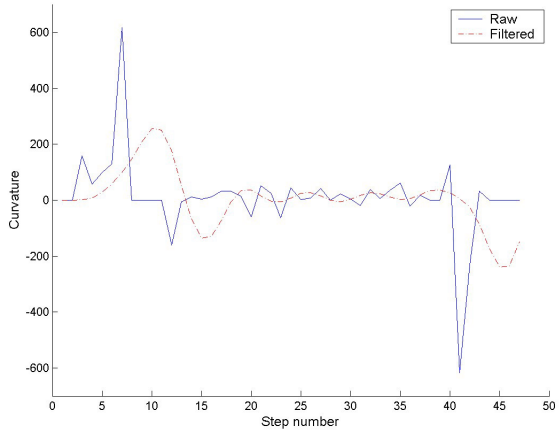

Fig. 12. Raw and filtered curvature.

For comparison to the traditional raster-scan image, in Figure 13 the local raster-scan data are plotted in a 575 nm square grid with each cell approximately 3 nm square. Here a weighted fill was used to fill in missing data in the matrix resulting in the artifacts on the right side of the image. Finally we note that each scan line was gathered in less than 10 ms. Thus, if the algorithm were implemented so as to avoid the long communication delays, the image would have been gathered in under 0.5 s.

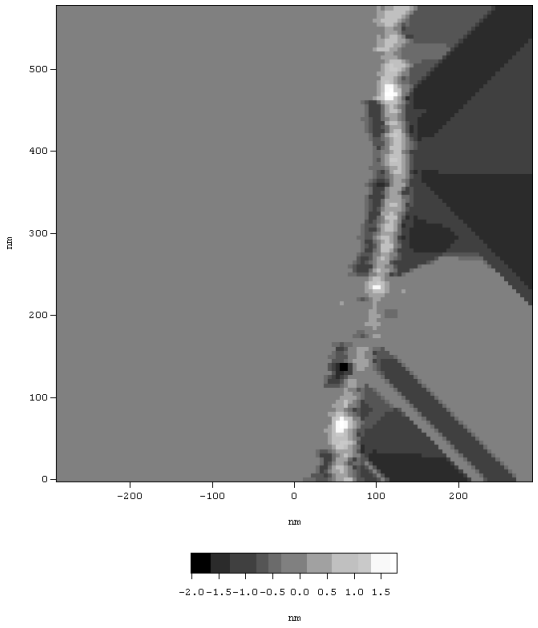

Fig. 13. Image of carbon nanotube using local raster-scan.

V. Conclusions

For samples which are string-like in nature, the standard raster-scan approach wastes a large amount of time imaging the substrate rather than the sample. In this paper we have presented a high-level algorithm to steer the tip along the sample, thereby imaging only those areas of interest. Modeling the sample as a planar curve whose evolution is given by the planar Frenet-Serret equations, feedback control is used to track the curve. By focusing the resolution of the microscope directly on those areas where it is needed, the time to gather an image is greatly reduced simply by reducing the area that needs to be scanned and the tip is protected from damage due to debris such as dust particles on the substrate.

We have presented both simulation results and a simple experiment with an atomic force microscope to illustrate the algorithm. While we have focused on AFM as the target application in this paper, the method is generally applicable to all scanning probe microscopy technologies.

VI. Acknowledgements

This work was supported in part by the Rowland Institute and by ARO ODDR&E MURI01 Grant No. DAAD19-01-1-0465, (Center for Communicating Networked Control Systems, through Boston University).

References

[1] M. Antognozzi, M.D. Szczelkun, A.D.L. Humphris, and M.J. Miles. Increasing shear force microscopy scanning rate using active quality-factor control. *Applied Physics Letters*, 82(17):2761–2763, 2003.

[2] D. Baselt. Atomic force microscopy. http://stm2.nrl.nvy.mil/how-afm/how-afm.html.

[3] G. Binnig, C.F. Quate, and Ch. Gerber. Atomic force microscope. *Physical Review Letters*, 56(9):930–933, 1986.

[4] G. Binnig, H. Rohrer, Ch. Gerber, and E. Weibel. Tunneling through a controllable vacuum gap. *Applied Physics Letters*, 40(2):178–180, 1982.

[5] E. Calabi, P.J. Olver, C. Shakiban, A. Tannenbaum, and S. Haker. Differential and numerically invariant signature curves applied to object recogonition. *International Journal of Computer Vision*, 26(2):107–135, 1998.

[6] H.C. Crenshaw, C.N. Ciampaglio, and M. McHenry. Analysis of the three-dimensional trajectories of organisms: Estimates of velocity, curvature, and torsion from positional information. *The Journal of Experimental Biology*, 203:961–982, 2000.

[7] A. Daniele, S. Salapake, M.V. Salapaka, and M. Dahleh. Piezoelectric scanners for atomic force microscopes: Design of lateral sensors, identification and control. In *Proceedings of the Americal Control Conference*, pages 253–257, 1999.

[8] U. Durig, D.W. Pohl, and F. Rohner. Near field optical scanning microscopy. *Journal of Applied Physics*, 59(10):3318–3327, 1986.

[9] M. Guthold, M. Bezanilla, D.A. Erie, B. Jenkins, H.G. Hansma, and C. Bustamante. Following the assembly of RNA polymerase-DNA complexes in aqueous solutions with the scanning force microscope. *Proceedings of the National Academy of Sciences*, 91:12927–12931, 1994.

[10] E. Justh and P.S. Krishnaprasad. Equilibria and steering laws for planar formations. *Systems and Control Letters*, 52:25–38, 2004.

[11] S. Kasas, N.H. Thomson, B.L. Smith, H.G. Hansma, X. Zhu, M. Guthold, C. Bustamante, E.T. Kool, M. Kashlev, and P.K. Hansma. *Escherichia coli* RNA polymerase activity observed using atomic force microscopy. *Biochemistry*, 36(3):461–468, 1997.

[12] A. Kornberg and T.A. Baker. *DNA Replication*. W.H. Freeman and Company, 1991.

[13] M. Mertz, O. Marti, and j. Mlynek. Regulation of a microcantilever response by force feedback. *Applied Physics Letters*, 62(19):2344–2346, 1993.

[14] G. Schitter, P. Menold, H.F. Knapp, F. Allgwer, and A. Stemmer. High performance feedback for fast scanning atomic force microscopes. *Review of Scientific Instruments*, 72(8):3320–3327, 2001.

[15] G. Schitter, R.W. Stark, and A. Stemmer. Fast contact-mode atomic force microscopy on biological specimen by model-based control. *Ultramicroscopy*, 100:253–257, 2004.

[16] A. Sebastian, D.R. Sahoo, and M.V. Salapaka. An observer based sample detection scheme for atomic force microscopy. In *Proc. of the* 42^{nd} *IEEE Conference on Decision and Control*, pages 2132–2137, 2003.

[17] Z. Shao, J. Mou, D.M. Czajkowsky, J. Yang, and J.Y. Yuan. Biological atomic force microscopy: What is achieved and what is needed. *Advances in Physics*, 45(1):1–86, 1996.

[18] M.B. Viani, T.E Schaeffer, G.T. Paloczi an L.I. Pietrasanta, B.L. Smith, J.B. Thompson, M. Richter, M. Rief, H.E. Gaub, K.W. Plaxco, A.N. Cleland, H.G. Hansma, and P.K. Hansma. Fast imaging and fast force spectroscopy of single biopolymers with a new atomic force microscope designed for small cantilevers. *Review of Scientific Instruments*, 70(11):4300–4303, 1999.

[19] F. Zhang, E. Justh, and P.S. Krishnaprasad. Boundary following using gyroscopic control. In *Proc. of the 43* rd *IEEE Conference on Decision and Control, to appear*, 2004.

[20] F. Zhang, A. O'Connor, D. Luebke, and P.S. Krishnaprasad. Experimental study of curvature-based control laws for obstacle avoidance. In *IEEE International Conference on Robotics and Automation*, pages 3849–3954, 2004.

[21] Z. Zhang, P.C. Hammel, and G.J. Moore. Application of a novel rf coil design to the magentic resonance force microscopy. *Review of Scientific Instruments*, 67(9):3307–3309, 1996.